Conformational Analysis of the *cis*- and *trans*-Adducts of the Pictet−Spengler Reaction. Evidence for the Structural Basis for the C(1)−N(2) Scission Process in the *cis*- to *trans*-Isomerization

Dongmei Han,[†] F. Holger Försterling,[†] Jeffrey R. Deschamps,[‡] Damon Parrish,[‡] Xiaoxiang Liu,[†] Wenyuan Yin,[†] Shengming Huang,[†] and James M. Cook*[,†]

Department of Chemistry, University of Wisconsin−Milwaukee, Milwaukee, Wisconsin 53211, and Laboratory for the Structure of Matter, Naval Research Laboratory, Washington, D.C. 20375

Received August 9, 2006

The stable conformations of both the *trans*- and *cis*-1,3-disubstituted N_b-benzyl stereoisomers of the Pictet−Spengler reaction have been determined by NMR spectroscopy and X-ray crystallography in order to better understand the C(1)−N(2) *cis*- to *trans*-isomerization process. In the N_a-H series, the chair conformation was preferred for the *trans*-isomer **3a**, while the *cis*-isomer **3b** existed predominantly in the boat form. However, in the N_a-methyl series (**1a**, **1b**, **2a**, **2b**), both the *cis* (**1b**, **2b**) and *trans* (**1a**, **2a**) diastereomers existed in the chair conformation to relieve the $A^{(1,2)}$-strain between the N_a-methyl function and the substituent at C(1). The difference in the preferred conformations of the *cis*-isomers in the N_a-H and N_a-methyl series (as compared to the preferred conformations in the *trans*-isomers) can be employed to understand the reduced rate of epimerization of *cis*-**2b** into *trans*-**2a** as compared to **3b** into **3a**. This provides the structural basis for the carbocation-mediated intermediate in the C(1)−N(2) scission process.

The Pictet−Spengler reaction,[1] which involves the cyclization of electron-rich aryl or heteroaryl groups onto imine or iminium ion electrophiles, has long been a standard method for the construction of both tetrahydro-β-carboline and tetrahydroisoquinoline systems. These ring systems are critical structural units that are commonly encountered in naturally occurring indole or isoquinoline alkaloids and include synthetic analogues with a wide diversity of important biological activity.[2] The enantiospecific Pictet−Spengler reaction has drawn widespread interest in both organic and medicinal chemistry.[3] Although important progress has been made recently,[3] the ideal solution to the catalytic enantiospecific Pictet−Spengler reaction has still not been reported. A study of the mechanism involved in the asymmetric Pictet−Spengler reaction of tryptophan alkyl esters may be valuable for the future design of other asymmetric Pictet−Spengler cyclizations, which are crucial in the construction of alkaloid core structures.

It is well documented that in nonacidic aprotic media N_b-benzyltryptophan alkyl esters undergo the Pictet−Spengler reaction with aldehydes to furnish the *trans*- and *cis*-diastereomers in an approximate ratio of 4:1, in which the *trans*-isomers predominate (Scheme 1).[4] Because of the presence of the two diastereomers, the separation of the isomers can be a tedious process especially for large-scale preparations. However, the thermodynamically more stable *trans*-isomer, a key chiral intermediate in the total synthesis of macroline/sarpagine/ajmaline indole alkaloids,[5] could be exclusively obtained by epimerization of the *cis*-stereoisomer or the mixture of the *cis*- and *trans*-isomers into the *trans*-diastereoisomer under acidic conditions (Table 1).[2c,d,6] Previously, three potential intermediates (Figure 1) were considered for this epimerization process based on earlier work on reserpine.[7] Among these intermediates, the *cis*- to *trans*-isomerization, which proceeds by protonation of the N_b-nitrogen atom, with concomitant cleavage of the C-1/N-2 bond is in better agreement with recent experiments.[6b,c] The resulting carbocation **7A**, after rotation of the C-1/C-9a carbon−carbon bond, can recyclize to provide the C-1 epimerized *trans*-diastereomer (Scheme 2). This carbocationic type of intermediate can be employed to explain the racemization of roeharmine upon isolation under acidic conditions, the racemization of harmine alkaloids, and the epimerization of reserpine into isoreserpine.[2a] Since alkoxy-substituted indole alkaloids (especially at positions 4 and 6 of the indole nucleus) might be prone to epimerization during isolation under the standard acidic conditions via such a carbocationic intermediate (see **7A**, Scheme 2), recent results on this process are reported here.

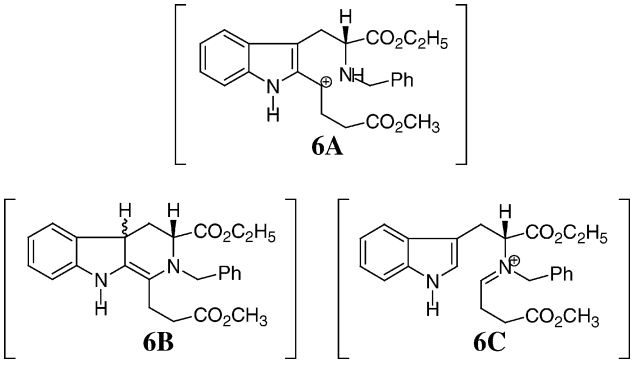

Figure 1. Proposed intermediates in the *cis*- to *trans*-epimerization.

It has been suggested that the conformation of the *cis*- and *trans*-stereoisomers plays an important role in the epimerization and that the formation of the carbocationic intermediate took place from a boat-like conformation.[8] The stable conformations of *trans*-**1a** and *cis*-**1b** isomers were studied several years ago.[9] It was concluded that the N_b-benzyl moiety and the substituent at C-1 assumed a *trans*-diaxial relationship in the preferred conformation in both *trans*-**1a** and *cis*-**1b**.[9] In the *trans*-isomer **1a**, the ester function at C-3 occupied the equatorial position, while in the *cis*-**1b** isomer, the axial orientation was preferred.[9] Outlined in this work are the results of conformational analysis and kinetic experiments, which support the boat-like conformation as the structural basis for the generation of the carbocationic intermediate in this *cis*- to *trans*-isomerization at C(1).

Results and Discussion

It was noticed that the epimerization of the mixture of *cis*- and *trans*-7-methoxy-substituted diastereomers occurred faster than its parent compound under acidic conditions.[6b] In order to further

* To whom correspondence should be addressed. Tel: 414-229-5856. Fax: 414-229-5530. E-mail: capncook@uwm.edu.
[†] University of Wisconsin−Milwaukee.
[‡] Naval Research Laboratory.

10.1021/np060391g CCC: $37.00
Published on Web 12/20/2006

Table 1. Epimerization of the *cis*-Isomers (**b**) into the *trans*-Diastereomers (**a**)

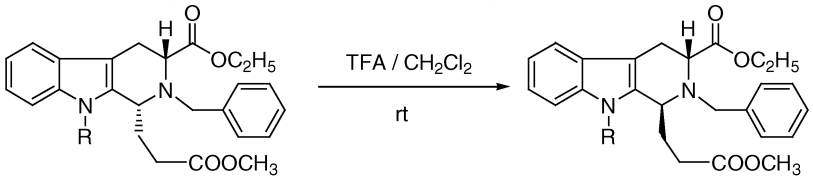

	approximate ratio of *cis*:*trans*[a]				
epimerization reactions	initial	30 min	7 h	3 days	10 days
2b → 2a	100:0			90:10	80:20
3b → 3a	100:0			45:55	0:100[b]
4b → 4a	100:0	86:14	0:100		
5b → 5a	100:0	0:100			
2a → 2b	0:100			0:100	0:100

[a] Ratio determined by analysis of the ^{1}H NMR spectrum of the crude reaction mixture. [b]The epimerization of **3b** went to completion in 7 days; analysis of the NMR data on day 10 indicated the ratio remained the same as day 7 (*cis*: *trans* 0:100). The TFA employed in these experiments was 1.5 equiv.

Scheme 1

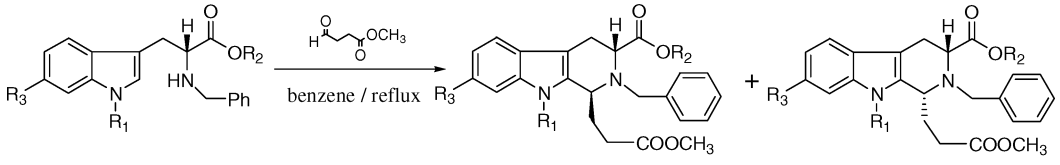

R_1 = R_2 = CH_3, R_3 = H	**1a**	**1b**
R_1 = CH_3, R_2 = CH_2CH_3, R_3 = H	**2a**	**2b**
R_1 = R_3 = H, R_2 = CH_2CH_3	**3a**	**3b**
R_1 = CH_3, R_2 = CH_2CH_3, R_3 = OCH_3	**4a**	**4b**
R_1 = H, R_2 = CH_2CH_3, R_3 = OCH_3	**5a**	**5b**

Scheme 2

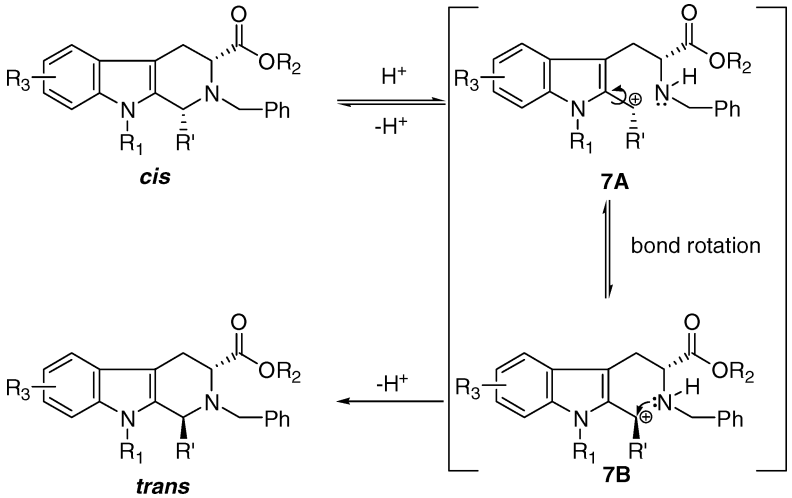

investigate the influence of substituents on the epimerization rate, a kinetic study was carried out, the results of which are listed in Table 1. Examination of the data in Table 1 illustrated that both the 7-methoxy-substituted *cis*-isomers (**4b**, **5b**) epimerized into the *trans*-diastereomers (**4a**, **5a**) much faster than the parent systems (**2b**, **3b**) isomerized into *trans*-**2a** and -**3a**, respectively. It was believed that the electrons on the 6-methoxy moiety of the indole contributed to the stabilization of the carbocationic intermediate **8** via the resonance structures **9** and **10** (Scheme 3). Furthermore, this is indirect support for the proposed mechanism of epimerization at C-1 of *cis*-1,2,3-trisubstituted tetrahydro-β-carbolines into the *trans*-isomers via the C(1)−N(2) cleavage process,[8] even though the retro-Pictet−Spengler reaction might also be accelerated in this case (Scheme 4). Even upon heating in excess acid at no time did any of the *cis*-N_a-H or -N_a-CH_3 diastereomers provide the related N_a-H or N_a-CH_3 N_b-benzyltryptophan alkyl esters. These reactions were monitored by TLC versus authentic material that would have arisen from a retro-Pictet−Spengler process. Only in the case of the N_a-substituted sulfonamide was the product of a retro-PS process observed.[6c] This provided indirect evidence that the iminium ion

Scheme 3

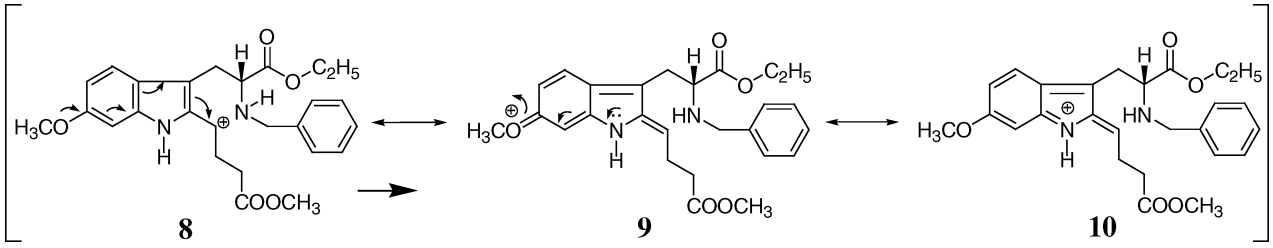

Scheme 4

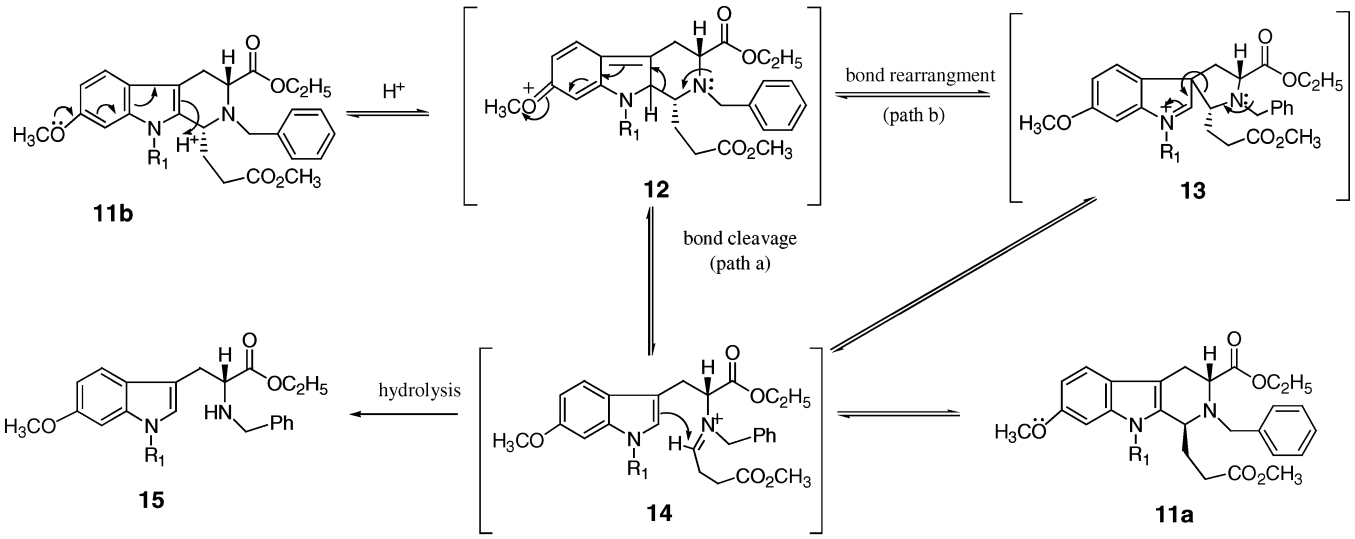

pathway was not operating in any of these epimerizations (N_a-H or N_a-methyl) with the exception of the deactivated N_a-sulfonamido-substituted series, wherein the carbocationic intermediate (C-1, N-2 scission) would have been destabilized by the electron withdrawal of the sulfonamide moiety.[6c]

Interestingly, analysis of the kinetic data also indicated that the N_a-methyl-substituted *cis*-diesters (**2b**, **4b**) epimerized at a much slower rate than the corresponding N_a-H-substituted cases (**3b**, **5b**). For example, the N_a-H *cis*-isomer **3b** epimerized completely into its *trans*-counterpart after 7 days. However, only about 20% of the corresponding *cis*-(TFA, CH_2Cl_2) N_a-methyl analogue had epimerized at day 10. In order to determine the final equilibrium ratio of this epimerization, the *trans*-diastereoisomer **2a** of **2b** was exposed to the same reaction conditions employed for **2b**. It was found that *trans*-**2a** remained unchanged after 10 days; no *cis*-**2b** was detected. Hence, it was deduced that the epimerization of **2b** → **2a** under these conditions of TFA/CH_2Cl_2 will go to completion eventually; that is the ratio of **2b**:**2a** would be 0:100 when the reaction time is long enough. This significant rate difference between the N_a-methyl and N_a-H series was observed in the parent system (**2b** vs **3b**) as well as in the 7-methoxy-substituted system (**4b** vs **5b**). The conformations of the diesters are believed to play an important role in this process.[8] In order to shed light on these observations and better understand the mechanism of the epimerization, the conformations of both the *cis*- and *trans*-1,2,3-trisubstituted tetrahydro-β-carbolines were determined.

The pure *cis*- and *trans*-diastereoisomers were initially prepared by condensing the D-N_b-benzyl-substituted tryptophan ethyl ester derivatives with methyl 4-oxobutanoate in refluxing benzene, and the diastereomers were separated by careful chromatography on silica gel. Each proton and carbon atom of the diastereomers was assigned via the examination of the 1D and 2D NMR spectra (see Figure 1, Supporting Information). The data are shown in Tables 2 and 3, respectively.

Both *trans*-diesters exhibited similar coupling constants and NOE patterns. From the ^{1}H NMR data for the *trans*-diesters **2a** and **3a**, the coupling constants observed between H-3 and H-4ax, H-4eq (^3J = 11.0, 4.9 Hz for **2a**, ^3J = 9.1, 5.2 Hz for **3a**) indicated that H-3 was located on the β-axial position of the C-ring. Furthermore, no NOE was detected between H-1 and H-3, while a cross-peak was observed between H-14 and H-3. These observations confirmed that in solution H-1 should be in the equatorial position. The *trans*-diesters **2a** and **3a** thus adopted similar stable conformations in solution in which the C-ring was a half-chair with an axial and equatorial substituent at C-1 and C-3, respectively. The NOE between H-4a and H-19 of **3a** was stronger than that between H-4e and H-19, which confirmed that the benzyl group was in an axial position on the same side of the ring as H-4a (see Figure 2 and Table 4). Distances between atoms were determined from the X-ray crystal structures or energy-minimized structures (Table 4). This arrangement was consistent with that reported for **1a**[2] and was confirmed by analysis of the X-ray crystal structure of **3a** (Figure 3), and consistent with other crystal structures of the *trans*-diastereoisomers.

Since the coupling constants between H-3 and H-4 ($^3J_{3,4ax}$ = 6.9 Hz, $^3J_{3,4eq}$ = 1.7 Hz) of **2b** are not very large, it was believed that the substituent at C-3 occupied the α-axial position. As in the case of the *trans*-diastereoisomers (see **2a** and **3a**), no NOE between H-1 and either H-3 or H-4ax or H-4eq was observed in the N_a-methyl *cis*-diester **2b** (see Figure 2 and Table 4). These data suggested that the C-ring in **2b** assumed a chair-like conformation similar to its *trans*-diastereomer **2a** with the C-1 proton located in the equatorial position. Moreover, NOEs were observed between the methylene protons of the benzyl group H-19 and both H-3 and

Table 2. ^{1}H NMR Data

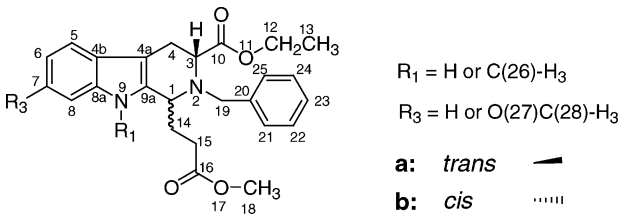

	2a	2b	3a	3b	4a	4b	5a	5b
H1	3.83 (dd, 4.9, 11.0)	3.95 (m)	3.96 (m)	3.95 (dd, 9.6, 5.4)	3.82 (m)	3.89 (m)	3.86 (m)	3.94 (m)
H3	4.11 (m)	3.89 (dd, 6.0, 2.0)	4.03 (dd, 9.1, 5.2)	3.86 (dd, 3.8, 6.0)	4.10 (d, 4.9, 11.0)	3.86 (dd, 6.9, 1.7)	3.97 (dd, 9.1, 4.9)	3.87 (m)
H4ax	3.18 (dd, 15.6, 11.0)	3.08 (dd, 16.0, 6.0)	3.18 (dd, 15.6, 9.1)	3.02 (dd, 15.6, 6.0)	3.16 (dd, 15.9, 11.0)	3.00 (ddd, 15.9, 6.9, 1.1)	3.09 (dd, 15.6, 9.1)	3.01 (dd, 15.7, 5.9)
H4eq	3.09 (dd, 15.6, 4.9)	3.38 (dd, 16.0, 2.0)	3.07 (dd, 15.6, 5.2)	3.25 (dd, 15.6, 3.8)	3.07 (dd, 15.9, 4.9)	3.25 (dd, 15.9, 1.7)	2.98 (dd, 15.6, 4.9)	3.24 (dd, 15.7, 3.9)
H5	7.62 (d, 7.7)	7.61 (d, 8.0)	7.59 (d, 7.7)	7.54 (d, 8.2)	7.50 (d, 8.5)	7.44 (d, 8.5)	7.40 (d, 8.5)	7.44 (d, 8.6)
H6	7.18 (t, 7.4)	7.16 (dt, 7.5,1.0)	7.17 (t, 7.4)	7.12 (ddd, 8.2,7.4,1.1)	6.87 (dd, 8.5, 2.2)	6.78 (dd, 8.5, 2.2)	6.79 (dd, 8.5, 2.2)	6.82 (dd, 8.6, 2.2)
H7	7.27 (m)	7.26 (dt, 8.2, 1.5)	7.22 (t, 7.7)	7.17 (ddd, 8.2,7.1,1.1)				
H8	7.35 (m)	7.34 (m)	7.37 (m)	7.35 (m)	6.85 (d, 2.2)	6.82 (d, 2.2)	6.85 (d, 2.2)	6.88 (d, 2.2)
H9			8.05 (brs)	8.04 (brs)			7.88 (brs)	7.99 (brs)
H12	4.34 (m)	4.10 (m)	4.28 (m)	4.10 (m)	4.35 (m)	4.05 (m)	4.23 (m)	4.13 (m)
H12′		4.21 (m)				4.19 (m)		
H13	1.42 (t, 7.1)	1.34 (t, 7.1)	1.34 (t, 7.1)	1.27 (t, 7.1)	1.43 (t, 7.1)	1.33 (t, 7.1)	1.31 (t, 7.1)	1.30 (t, 7.1)
H14	1.89 (m)	1.60 (m)	2.01 (m)	1.96 (m)	2.04 (m)	1.53 (m)	1.95 (m)	1.91 (m)
H14′	2.04 (m)	1.98 (m)	2.12 (m)	2.12 (m)	1.89 (m)	1.94 (m)	2.05 (m)	2.02 (m)
H15	2.45 (m)	2.55 (m)	2.36 (m)	2.53 (m)	2.46 (m)	2.57 (m)	2.32 (m)	2.52 (m)
H15′	2.65 (m)	2.88 (m)	2.48 (m)		2.65 (m)	2.80 (m)	2.42 (m)	2.60 (m)
H18	3.51 (s)	3.59 (s)	3.55 (s)	3.59 (s)	3.53 (s)	3.57 (s)	3.51 (s)	3.62 (s)
H19	3.42 (d, 13.5)	3.80 (d, 13.5)	3.62 (d, 13.7)	3.88 (d, 13.7)	3.44 (d, 13.2)	3.79 (d, 13.2)	3.57 (d, 13.7)	3.91 (d, 14.2)
H19′	3.87 (d, 13.5)	3.95 (d, 13.5)	3.91 (d, 13.7)	3.97 (d, 13.7)	3.87 (d, 13.2)	3.94 (d, 13.2)	3.85 (d, 13.7)	3.99 (d, 14.2)
H21, 25	7.39 (d, 7.1)	7.46 (d, 7.5)	7.41 (d, 7.4)	7.44 (d, 7.4)	7.42 (d, 7.1)	7.48 (d, 7.1)	7.36 (d, 7.4)	7.47 (d, 7.3)
H22, 24	~7.35 (m)	~7.38 (m)	~7.36 (m)	~7.40 (m)	7.36 (m)	7.38 (m)	~7.31(m)	~7.37 (m)
H23	7.30 (m)	7.33 (m)	7.30 (m)	7.28 (m)	7.31(m)	7.32(m)	7.25(m)	7.31(m)
H26	3.69 (s)	3.70 (s)			3.65 (s)	3.62 (s)		
H28					3.96 (s)	3.91 (s)	3.85 (s)	3.88 (s)

Table 3. ^{13}C NMR Data

	2a	2b	3a	3b	4a	4b	5a	5b
C1	53.28	54.23	54.60	56.10	53.75	54.88	55.07	56.25
C3	56.20	57.62	56.75	58.95	56.67	57.87	57.20	59.07
C4	20.25	18.10	21.17	19.92	20.72	18.16	21.64	20.05
C4a	106.39	104.86	107.50	106.56	106.70	105.01	107.79	106.42
C4b	126.58	126.62	126.99	126.95	121.46	121.44	121.87	121.45
C5	118.21	118.33	118.17	118.22	119.17	118.91	119.08	118.80
C6	119.16	118.99	119.50	119.37	109.06	108.42	109.40	108.88
C7	121.35	121.33	121.77	121.70	156.69	156.63	156.76	156.32
C8	108.96	108.86	110.93	110.79	93.67	93.21	95.51	95.02
C8a	137.48	137.55	136.24	136.08	138.62	138.71	137.42	136.88
C9a	135.78	134.66	134.24	133.36	135.01	133.89	133.36	132.10
C10	172.99	173.69	172.97	173.36	173.45	174.15	173.42	173.52
C12	60.97	61.02	60.81	60.84	61.37	61.31	61.21	60.87
C13	14.41	14.06	14.35	14.03	14.84	14.91	14.79	14.15
C14	27.97	29.15	28.98	29.16	28.48	29.58	29.45	29.20
C15	29.64	30.22	29.87	30.37	30.08	30.37	30.33	30.41
C16	174.00	174.33	174.34	173.44	174.48	174.43	174.80	174.64
C18	51.34	51.41	51.50	51.52	51.76	51.54	51.91	51.56
C19	52.77	61.31	53.33	59.21	53.19	61.59	53.74	59.26
C20	139.37	139.03	139.40	139.02	139.88	139.78	139.91	139.13
C21,25	129.25	129.36	129.14	128.94	129.78	129.51	129.55	128.98
C22,24	128.20	128.42	128.25	128.31	128.61	128.67	128.65	128.34
C23	127.01	127.38	127.09	127.24	127.41	127.54	127.48	127.25
C26	29.78	29.77			30.25	30.11		
C28					56.38	56.03	56.26	55.82

H-4a, which suggested that the benzyl group assumed a β-axial position (see Figure 2, Table 4; see also Figure 2, Supporting Information). This structure was similar to the conformation found in *cis*-**1b**[2] and was also confirmed by an X-ray crystal structure (Figure 3). This is also in agreement with the reported X-ray crystal structure of the *cis*-N_a-methyl N_b-benzyl diester **16**.[10]

In the case of the parent N_a-H *cis*-compound **3b**, the coupling constants ^{3}J(H-3, H-4ax) and ^{3}J(H-3, H-4eq) were measured as 6.0

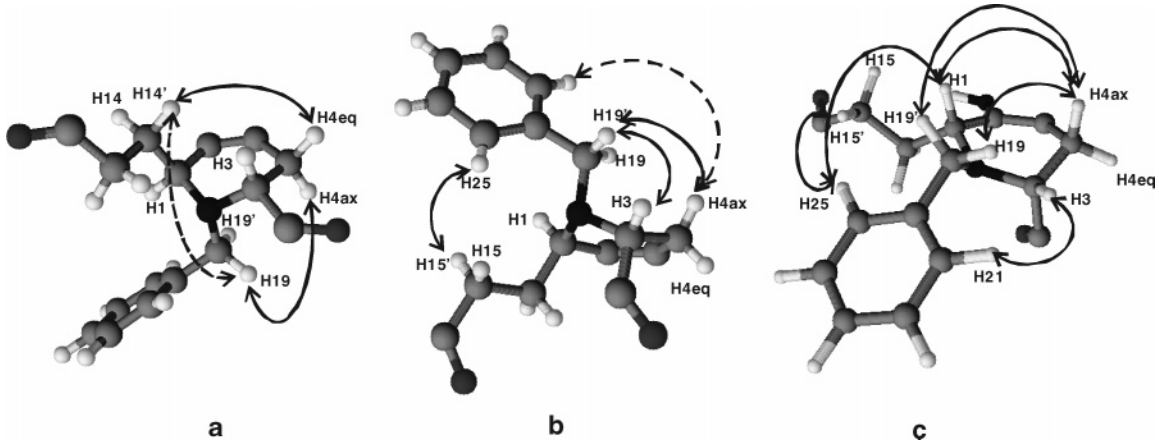

Figure 2. Illustration of observed NOEs in the various structures. (a) Crystal structure of **3a** (*trans*, half-chair), (b) crystal structure of **2b** (*cis*, half-chair), (c) modeled structure of **3b** (*cis*, boat). This structure was obtained from a minimized boat structure by twisting the ring into a boat conformation with Insight software. In all cases the indole ring and the methoxy/ethoxy groups are omitted for clarity. Observed NOEs are indicated by double arrows. Dashed lines (---) indicate NOEs that are observed but are not supported by the rigid crystal structure. Modeling with minimized half-chair conformations has shown that low-energy substituent conformations exist where these distances are below 3.7 Å.

Table 4. Selected Interatomic Distances in **3a**, **2b**, and **3b**[a]

	3a (*trans*, half-chair)		**2b** (*cis*, half-chair)		**3b** (*cis*, boat)
distance	model	crystal	model	crystal	model
H-1 and H-3	3.78	3.71	4.26	3.94	3.85
H-1 and H-4ax	4.42	4.86	4.90	4.18	**3.28**
H-1 and H-4eq	4.80	4.64	4.28	4.62	***4.50***
H-3 and H-14	3.438, 3.942	2.29,3.78	4.09	3.81	4.43
H-3 and H-21 (H-25)	2.14	4.16	3.09	3.94	2.60
H-3 and H-19	2.97,3.67	3.84,3.58	**2.87**, **3.68**	**2.08**, **2.87**	1.89
H-14 and H-4ax	4.68	4.61	4.21	4.52	5.12
H-14 and H-4eq	**3.90**	**3.89**	4.74	3.97	5.46
H-19 and H-4ax	***4.43***	**2.86**, **2.72**	**2.87**	**2.81**, **2.58**	**3.02**, **3.85**
H-14 and H-19	**3.18**	***4.42***	4.39	4.38	**3.18**
H-21 (H-25) and H-1	2.14	4.16	4.19	3.04,3.73	**3.59**
H-21 (H-25) and H-4ax	3.83	5.05,5.18	**3.62**	***4.78***	4.80
H-21 (H-25) and H-15	3.63	3.16	**2.63**	**2.83**, **2.50**	**2.02**, 3.71

[a] For **3a** and **2b** both numbers for the crystal structure and for a minimized half-chair conformation are shown. For **3b** an idealized boat conformation was produced with Insight, as no boat conformation could be obtained by minimization. NOEs shown in Figure 2 are indicated in **bold**. The H-1−H-4eq NOE in **3b** is weak and most likely due to spin diffusion. For some flexible substituents, the distances can vary between the crystal and modeled data.

and 3.8 Hz, respectively, which indicated that H-3 also assumed an equatorial position in the C-ring (see Table 5). On the other hand, the pattern of the NOEs in the N_a-H *cis*-isomer **3b** was different from that of the *cis*-N_a-CH_3 analogue **2b**. In *cis*-**3b**, NOEs were observed between H-1 and both the H-4ax and H-4eq (see Figure 2 and Table 4; see also Figure 3, Supporting Information). These NOEs were not observed in the N_a-methyl *cis*-diester **2b**. Further data on the dihedral angles in the C-ring of **3b** were obtained by measurement of the vicinal $^3J_{CH}$ coupling constants derived from an HSQMBC spectrum.[11] The J values of 8 and 0.5 Hz for ^3J(H-4^{ax}, C-10) and ^3J(H-4^{eq}, C-10), respectively, and ^3J(H-3, C-4A) = 5.5 Hz indicated that the ester (C-10) adopted an axial orientation and H-3 an equatorial position. In similar fashion, the value of ^3J(H-1, C-4A) ≈ 0.5 Hz was consistent with an axial position for H-1. Analysis of these data indicated that the preferred conformation of **3b** was in agreement with the interpretation of the NOEs, which indicated a boat-like C-ring, as indicated in Figure 2. Similar coupling constants were found in *cis*-**5b**, and analysis of those data indicated that the 7-methoxy-substituted **5b** adopted a similar boat conformation as that preferred in the 7-H parent **3b**, as expected.

This was a key finding since the stable conformation of *cis*-**3b** had not previously been reported; consequently, the preference for the half-boat conformation for these types of *cis*-conformers had also not been proposed.[2] Previously, the only report on the stable conformation for *cis*-N_b-benzyl-1,2,3-trisubstituted tetrahydro-β-carbolines in the N_a-H series was on *cis*-1-cyclohexyl-2(N)benzyl-3-methoxycarbonyl-1,2,3,4-tetrahydro-β-carboline.[10] In this diester, the 1,3-diaxial conformation was regarded as the stable one.[10]

In addition to the information from conformational analysis, examination of the specific rotations in Table 5 illustrated an interesting phenomenon. If either R_2 or R_3 is changed in these molecules, the specific rotations do not change very much (see **3b**, **6b**, **5b**); however, in the case of the N_a-H (**3b**, **6b**, **5b**, half-boat conformation) versus the N_a-methyl analogues (**1b**, **2b**, **4b**, chair-like conformation), the rotations differ significantly. This confirmed the close relationship between the conformation and specific rotation of those compounds.

The elucidation of the difference in the conformation of the C-ring of the N_a-H *cis*-isomer **3b** in comparison to its N_a-CH_3 analogue **2b** provided an opportunity for a better understanding of the epimerization mechanism and revealed a structural basis for the generation of the carbocationic intermediate. Analysis of the interactions in the *cis*-diastereomers indicated that two major types of repulsive interactions should contribute to the difference in the conformations: $A^{(1,2)}$ strain[2b,c,12] and 1,3-diaxial interactions. It is well documented that the group at the allylic position in a cyclohexene ring prefers to occupy a quasiaxial position to release $A^{(1,2)}$ strain, while substituents in chair conformations tend to orient themselves in equatorial positions to reduce the butane gauche (1,3-diaxial) interactions. No doubt, the larger the size of the groups, the stronger the interactions.

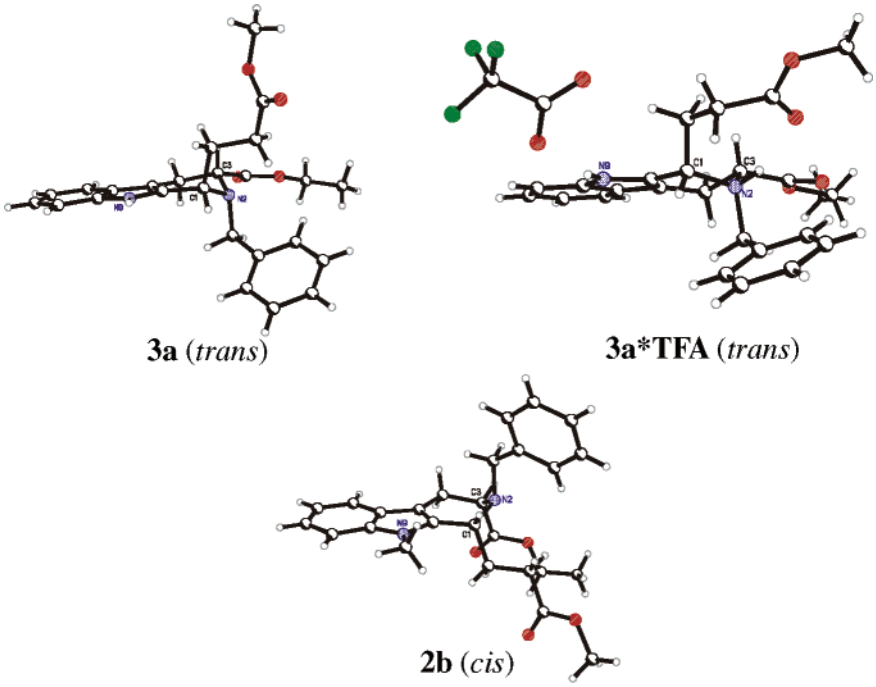

Figure 3. Illustrations from the X-ray crystal structure of **2b** (bottom), **3a** (top left), and **3a**·TFA salt (top right).

Table 5. Specific Rotations of Different *cis*-Diesters

	$R_1 = H$	$R_1 = CH_3$
$R_2 = CH_3$, $R_3 = H$	−1.3 (**6b**)[9b]	+20.0 (**1b**)[9d]
$R_2 = C_2H_5$, $R_3 = H$	−3.3 (**3b**)	+20.0 (**2b**)
$R_2 = C_2H_5$, $R_3 = OCH_3$	−2.7 (**5b**)	+19.3 (**4b**)

Clearly, the balance between these two interactions would determine the stable conformation of the stereoisomers (Scheme 4). In the N_a-CH_3 *cis*-diesters **1b** and **2b**, the equilibrium favored the chair-like conformer (**A**), despite 1,3-diaxial interactions that existed in this conformation. In this conformer, the axial orientation of the substituent at C-1 minimized the interaction between it and the bulky N_a-CH_3 group. An increase in the size of the ester group at R_2 from CH_3 (**1b**) to CH_3CH_2 (**2b**) did not alter the stable conformations. It was thus concluded that $A^{(1,2)}$ strain exerted a controlling effect over 1,3-diaxial repulsions on the favored conformation in these *cis*-diastereomers. This finding was further supported by the conformation of the N_a-H *cis*-diester **3b**. Since a hydrogen atom is small (see **3b**) as compared to the methyl substituent at the N_a-indole position, the $A^{(1,2)}$ strain was relatively weak in **3b**. Hence the repulsion between the 1,3-diaxial substituents became the dominant force and resulted in the half-boat conformer in **3b** to reduce these interactions. In contrast, the cyclohexyl group at C(1) in the *cis*-isomer of the compound reported by Bailey et al.[10] is a very bulky group, and the $A^{(1,2)}$ strain between it and the N_a-H group presumably favored the axial position for this substituent. The result was a 1,3-diaxial conformation for this diester.[10] In brief, the *cis*-N_a-H isomers could exist in either the half-chair or half-boat conformations depending on the size of the substituent at C-1. In the present work, the *cis*-isomers in the N_a-H series [C-1 substituent; propylmethyl ester group] clearly existed in the half-boat conformation on the basis of the NMR data.

In the presence of TFA, the protonation of the N_b nitrogen atom would be expected to occur from the same face as the lone pair of electrons and maintain the conformation of the isomers as that in the free base. This was supported by the X-ray crystal structure of **3a**·TFA (Figure 3). In order to cleave the C(1)−N(2) bond to undergo the epimerization, it was believed[8] that the orbital of this bond should overlap well with the π-bond of the 2,3-indole system. Ideally, when this C(1)−N(2) bond becomes parallel to the π-electron system of the indole ring, the π-electrons would be able

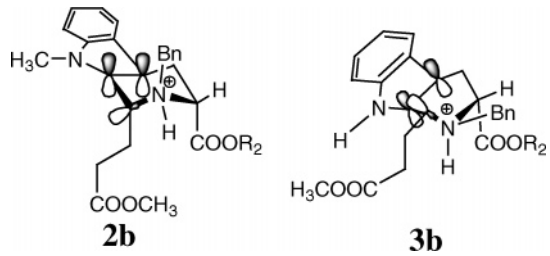

Figure 4. Proposed electronic orbital alignment of *cis*-**2b** and -**3b**.

Scheme 5

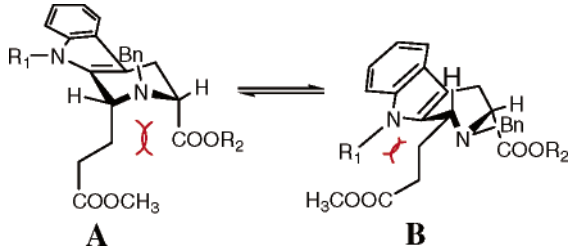

to delocalize into the σ*-orbital of the C(1)−N(2) bond and stabilize the developing carbocationic intermediate. In the boat-like conformation in **3b** (Figure 4), the σ*-orbital is approximately parallel, respectively with the π-system of the indole double bond to stabilize the C(1)−N(2) bond cleavage by orbital overlap. However, in the half-chair conformation such as that found in **2b**, the σ*-orbital would be perpendicular to the π-system; consequently, generation of the carbocationic intermediate would be less efficient. It was thus believed that the transition states for the bond-breaking process were best achieved from the boat-like conformations of the diesters. This is regarded as the structural basis for the carbocationic mediated epimerization mechanism of the *cis*-isomers into the *trans*-diastereomers.

The chair-like conformers of the isomer that undergoes the epimerization have to flip into a boat-like conformation to facilitate the C(1)−N(2) scission via the carbocationic intermediate; otherwise the rate of epimerization will be retarded. In the four possible conformations for the *cis*-isomers (Figure 5), conformers **A** and **B** are the two low-energy conformations for **2b** and **3b**, as determined

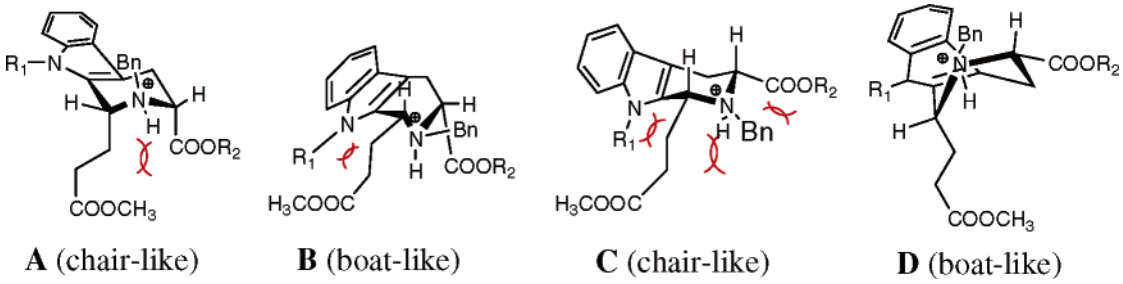

Figure 5. Four possible low-energy conformations for *cis*-diesters.

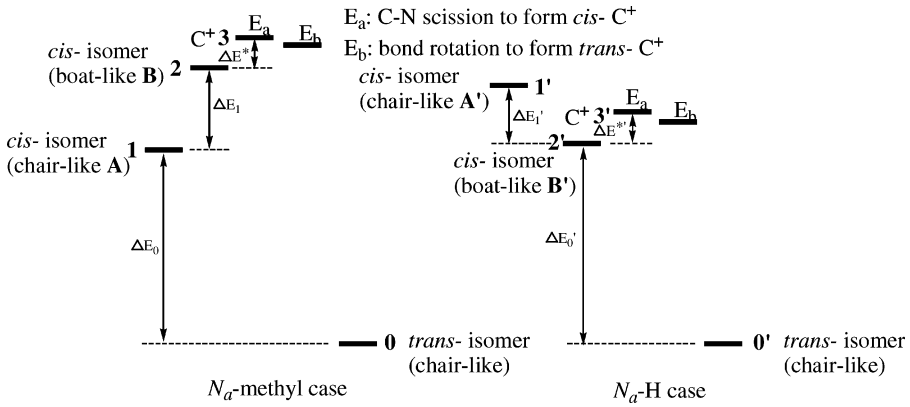

Figure 6. Approximate energy diagram for the epimerization in both the N_a-CH_3 (left) and N_a-H (right) cases.

Scheme 6

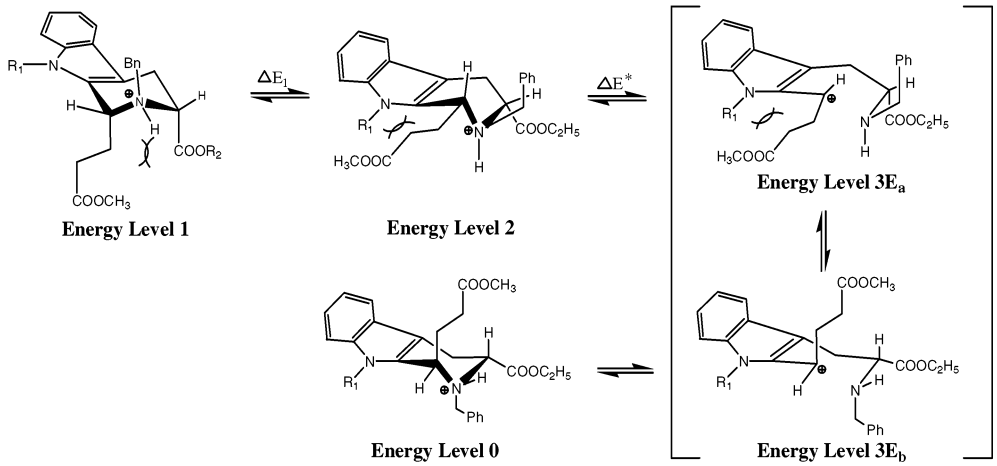

by NMR spectroscopy and X-ray crystallography. Conformations **C** and **D** can be ruled out by the NMR data of **3b**, since they contain the substituent at C-10 in an equatorial position and H-3 in an axial position, while HSQMBC data indicated that couplings H-4a,e−C-10 are consistent with an axial position for the C-10 substituent in **3b**. Furthermore, structure D involved an axial C-1 group and an equatorial H-1, contrary to the NOE data, which indicated that H-1 in **3b** was axial. It was, therefore, assumed that these latter conformations are not relevant in the analysis. Conformer **B** is the preferred conformation required in the transition state for the epimerization. Because of the existence of the $A^{(1,2)}$ strain, there is a value for the energy barrier (ΔE_1) for the *cis*-N_a-methyl diester **2b** to flip into a half-boat conformer **B** from the ground state half-chair conformation **A**. However, for *cis*-isomer **3b** the boat-like conformation is the ground state. There is no need to overcome ΔE_1 before cleavage of the C(1)−N(2) bond, as required in **2b**. Thus, the epimerization of N_a-methyl **2b** to **2a** requires a higher energy barrier and proceeds slower than the *cis*-N_a-H diester **3b** to *trans*-**3a** isomerization. Since the equilibrium was always on the side of the *trans*-isomer, the ground state energy difference (ΔE_0) was sufficient in both cases (N_a-methyl and N_a-H) to drive the equilibrium (*cis* → *trans*) to completion. An approximate energy diagram and a scheme for the epimerization process are shown in Figure 6 and Scheme 6.

Conclusion

The stable conformations of both the *trans*- and *cis*-N_b-benzyl-1,3-disubstituted diastereomers in the N_a-H and N_a-CH_3 series of Pictet−Spengler adducts were determined by analysis of NMR spectroscopy and X-ray crystallography. In most of the diastereoisomers (**2a**, **2b**, **3a**), the half-chair C-ring was found in the preferred conformer except in the important N_a-H *cis*-diesters **3b** and **5b**, which adopted a boat-like C-ring. The determination of these stable conformations in **3b** and **5b** is new. Second, $A^{(1,2)}$ strain was regarded as a relatively strong interaction in these types of 1,2,3-trisubstituted tetrahydro-β-carbolines, although in other cases it has been regarded as a weak interaction.[10] It influenced the preferred conformations to a greater degree than 1,3-diaxial interactions. Hence in all of the preferred conformations, $A^{(1,2)}$ strain was either initially weak or minimized. The thermodynamic effects alone can account for the 100% *trans*-diastereoselectivity observed in the asymmetric Pictet−Spengler reaction under acidic conditions;

however, the difference in rates in the epimerization process can be understood via analysis of the conformations of the diastereomers. The *cis*-compounds **3b** and **5b**, which exist in a boat-like conformation in which the σ^*-orbital of the C(1)−N(2) bond is approximately parallel with the π-system of the indole ring, epimerized much faster than the half-chair N_a-CH_3 cases. In agreement with this orbital overlap, the 7-methoxy-substituted *cis*-isomers epimerized much faster than the N_a-H (parent) compounds.[6b,c,8] These findings support the boat-like transition states proposed earlier[8] and provide support for the existence of the carbocationic intermediate. This conformational evidence, when combined with previous results,[6] supports the epimerization mechanism mediated by this carbocationic intermediate.[6] This study may provide a means for the future design of asymmetric Pictet−Spengler reactions.

Experimental Section[13]

General Procedure for the Preparation of Both the *trans*- and *cis*-Diastereoisomers. The optically active N_b-benzyl-D-tryptophan ethyl ester (16.2 mmol) and methyl 4-oxobutanoate (1.15 equiv) were dissolved in C_6H_6 (100 mL) in a round-bottom flask that was equipped with a Dean−Stark trap and a reflux condenser. The reaction mixture was degassed and heated to reflux under argon until all of the tryptophan ethyl ester was consumed (TLC). The solvent was removed under reduced pressure, and the crude residue was purified by careful column chromatography (silica gel, gradient elution, EtOAc/hexane = 20:1, 15:1, 10:1, 8:1) to provide the pure *trans*-diastereomer and pure *cis*-isomer, respectively.

General Procedure for the Kinetic Epimerization Experiments. The TFA (1.5 equiv) was added to the diastereoisomer, which had been dissolved in dry CH_2Cl_2 (0.375 mol/mL), and the mixture was stirred at rt under argon. At each data point (as indicated in Table 1), a small amount of reaction solution was diluted with EtOAc. The organic layer was stirred with a cold dilute aqueous solution of $NaHCO^3$ and dried (Na_2SO_4). The solvent was removed under reduced pressure and the residue was dissolved in CD_2Cl_2 or $CDCl_3$ to determine the ratio of the two diastereoisomers by ^{1}H NMR spectroscopy.

Acknowledgment. The authors thank the NIMH (MH-46851) and NSF (instrumentation grant NSF-9512622) for support of this work. Moreover, the authors acknowledge NIDA and ONR for support of the X-ray crystallography.

Supporting Information Available: X-ray crystallographic data, NOE spectra (Figures 2, 3, and 8), proton NMR spectra (Figure 1), and ^{13}C NMR spectra of **2a**, **2b**, **3a**, and **3b** (Figures 4−7) as well as the characterization of **2a**, **2b**, **3a**, **3b**, **4a**, **4b**, **5a**, and **5b** are available free of charge via the Internet at http://pubs.acs.org.

References and Notes

(1) (a) Pictet, A.; Spengler, T. *Ber. Dtsch. Chem. Ges.* **1911**, *44*, 2030−2036. (b) Tatsui, G. *Yakugaku Zasshi* **1928**, *48*, 453−459. (c) Whaley, W. M.; Govindachari, T. R. In *Organic Reactions*; Adams, R., Ed.; John Wiley and Sons: New York, 1951; Vol. VI, pp 151−190. (d) Cox, E. D.; Cook, J. M. *Chem. Rev.* **1995**, 1797−1842.

(2) Examples utilizing the Pictet−Spengler reaction. (a) Czerwinski, K. M.; Cook, J. M. In *Advances in Heterocyclic Natural Products Synthesis*; Pearson, W., Ed.; JAI Press: Greenwich, CT, 1996; Vol. 3, pp 217−277. (b) Ashley, E. R.; Cruz, E. G.; Stoltz, B. M. *J. Am. Chem. Soc.* **2003**, *125*, 15000−15001. (c) Niesen, T. E.; Meldal, M. *J. Org. Chem.* **2004**, *69*, 3765−3773. (d) Bunin, B. A.; Dener, J. M.; Kelly, D. E.; Paras, N. A.; Tario, J. D.; Tushup, S. P. *J. Comb. Chem.* **2004**, *6*, 487−496.

(3) (a) Ungemach, F.; DiPierro, M.; Weber, R.; Cook, J. M. *J. Org. Chem.* **1981**, *46*, 164−168. (b) Czarnocki, Z.; Suh, D.; MacLean, D. B.; Hultin, P. G.; Szarek, W. A. *Can. J. Chem.* **1992**, *70*, 1555−1561. (c) Reddy, M. S.; Cook, J. M. *Tetrahedron Lett.* **1994**, *35*, 5413−5416. (d) Waldmann, H.; Schmidt, G.; Henke, H.; Burkard, M. *Angew. Chem., Int. Ed. Engl.* **1995**, *34*, 2402−2403. (e) Yamada, H.; Kawate, T.; Matsumizu, M.; Nishida, A.; Yamaguchi, K.; Nakagawa, M. *J. Org. Chem.* **1998**, *63*, 6348−6354. (f) Gremmen, C.; Willemse, B.; Wanner, M. J.; Koomen, G-J. *Org. Lett.* **2000**, *2*, 1955−1958. (g) Taylor, M. S; Jacobsen, E. N. *J. Am. Chem. Soc.* **2004**, *126*, 10558−10559. (h) Seayad, J; Seayad, A. M.; List, B. *J. Am. Chem. Soc.* **2006**, *128*, 1086−1087.

(4) (a) Sandrin, J.; Soerens, D.; Mokry, P.; Cook, J. M. *Heterocycles* **1977**, *6*, 1133−1139. (b) Soerens, D.; Sandrin, J.; Ungemach, F.; Mokry, P.; Wu, G. S.; Yamanaka, E.; Hutchins, L.; DiPierro, M.; Cook, J. M. *J. Org. Chem.* **1979**, *44*, 535−545. (c) Cain, M.; Campos, O.; Guzman, F.; Cook, J. M. *J. Am. Chem. Soc*. **1983**, *105*, 907−913.

(5) (a) Bi, Y.; Zhang, L. H.; Hamaker, L. K.; Cook, J. M. *J. Am. Chem. Soc.* **1994**, *116*, 9027−9041. (b) Yu, P.; Wang, T.; Li, J.; Cook, J. M. *J. Org. Chem.* **2000**, *65*, 3173−3191. (c) Wang, T.; Cook, J. M. *Org. Lett.* **2000**, *2*, 2057−2059. (d) Liu, X.; Deschamps, J. R.; Cook, J. M. *Org. Lett.* **2002**, *4*, 3339−3342.

(6) (a) Zhang, L. H.; Gupta, A. K.; Cook, J. M. *J. Org. Chem*. **1989**, *54*, 4708−4712. (b) Cox, E. D.; Li, J.; Hamaker, L. K.; Yu, P.; Cook, J. M. *Chem. Commun*. **1996**, 2477−2478. (c) Cox, E. D.; Hamaker, L. K.; Li, J.; Yu, P.; Czerwinski, K. M.; Deng, L.; Bennett, D. W.; Cook, J. M.; Watson, W. H.; Krawiec, M. *J. Org. Chem*. **1997**, *62*, 44−61.

(7) Gaskell, A. J.; Joule, J. A. *Tetrahedron* **1967**, *23*, 4053−4063.

(8) (a) Liu, X., Ph.D. Thesis, University of Wisconsin−Milwaukee, 2002. (b) Han, D.; Liu, X.; Cook, J. M. 227th American Chemical Society National Meeting, Anaheim, CA, March 28−April 1, 2004, ORGN-485.

(9) (a) Shimizu, M.; Ishikawa, M.; Komoda, Y.; Nakajima, T.; Yamaguchi, K.; Yoneda, N. *Chem. Pharm. Bull.* **1984**, *32*, 463−474. (b) Shimizu, M.; Ishikawa, M.; Komoda, Y.; Nakajima, T.; Yamaguchi, K.; Sakai, S. *Chem. Pharm. Bull.* **1984**, *32*, 1313−1325. (c) Zhang, L.H.; Cook, J. M. *Heterocycles* **1988**, *27*, 1357−1363. (d) Zhang, L. H. Ph.D. Thesis, University of Wisconsin−Milwaukee, 1990. (e) Li, J. Ph.D. Thesis, University of Wisconsin−Milwaukee, 1999.

(10) Bailey, P. D.; Hollinshead, S. P.; Mclay, N. R.; Morgan, K.; Palmer, S. J.; Prince, S. N.; Reynolds, C. D.; Wood. S. D. *J. Chem. Soc., Perkin Trans. 1* **1993**, 431−439.

(11) Williamson, R. T.; Marquez, B. L.; Gerwick, W. H.; Köver, K. E. *Magn. Reson. Chem.* **2000**, *38*, 265−273.

(12) (a) Johnson, F. *Chem. Rev.* **1968**, *68*, 375−413. (b) Casy, A. F; Beckett, A. H.; Iorio, M. A. *Tetrahedron* **1966**, *22*, 2751−2760. (c) Beckett, A. H.; Casy, A. F.; Iorio, M. A. *Tetrahedron* **1966**, *22*, 2745−2750.

(13) Please see the Supporting Information for materials and general instrumentation.

NP060391G